energies

MDPI

Review

A Review on Kinetic Energy Harvesting with Focus on 3D Printed Electromagnetic Vibration Harvesters

Philipp Gawron *, Thomas M. Wendt, Lukas Stiglmeier, Nikolai Hangst and Urban B. Himmelsbach

Department of Business and Industrial Engineering, Offenburg University of Applied Sciences, Klosterstraße 18, 77723 Gengenbach, Germany; thomas.wendt@hs-offenburg.de (T.M.W.); lukas.stiglmeier@hs-offenburg.de (L.S.); nikolai.hangst@hs-offenburg.de (N.H.); urban.himmelsbach@hs-offenburg.de (U.B.H.)

* Correspondence: philipp.gawron@hs-offenburg.de

Abstract: The increasing amount of Internet of Things (IoT) devices and wearables require a reliable energy source. Energy harvesting can power these devices without changing batteries. Three-dimensional printing allows us to manufacture tailored harvesting devices in an easy and fast way. This paper presents the development of hybrid and non-hybrid 3D printed electromagnetic vibration energy harvesters. Various harvesting approaches, their utilised geometry, functional principle, power output and the applied printing processes are shown. The gathered harvesters are analysed, challenges examined and research gaps in the field identified. The advantages and challenges of 3D printing harvesters are discussed. Reported applications and strategies to improve the performance of printed harvesting devices are presented.

Keywords: energy harvesting; 3D printed; vibration harvester; electromagnetic; hybrid

Citation: Gawron, P.; Wendt, T.M.; Stiglmeier, L.; Hangst, N.; Himmelsbach, U.B. A Review on Kinetic Energy Harvesting with Focus on 3D Printed Electromagnetic Vibration Harvesters. *Energies* **2021**, *14*, 6961. https://doi.org/10.3390/en14216961

Academic Editor: Dibin Zhu

Received: 22 September 2021
Accepted: 18 October 2021
Published: 22 October 2021

1. Introduction

Energy harvesting is the utilisation of ambient energy in order to power electronics such as wireless sensor nodes (WSN) or wearables without the need of batteries [1–3]. This allows to operate the node over a much longer time period compared to battery-powered devices along with lower maintenance efforts. Furthermore, the low-maintenance requirements allow to operate these WSNs in environments with limited or no accessibility [4,5]. Energy harvesting can be categorised into four types of energy sources: solar/light, mechanical motion/vibration, thermoelectricity and electromagnetic radiation. Each type of energy source has different concepts to convert the ambient energy into electrical energy [1]. Testing different energy harvesters often requires specific power conditioning depending on the type of harvester. In [6], a reconfigurable power management was presented, allowing fast adaptation of the power management.

Solar energy is converted into electrical energy via solar panels [4,5]. Compared to outdoor applications the indoor available energy is 10 to 100 times lower [7]. The light's spectral composition and the applied photovoltaic cell significantly impact the generated power, even if the same illuminance level is given [8]. Thermoelectric generators (TEG) utilise the Seebeck-effect to convert thermal into electrical energy [9]. The TEG's hot side is mounted on a heat source and the cold side on a heat sink. A temperature gradient between both sides creates an electric voltage [1,10]. RF harvesting utilises electromagnetic (EM) radiation in the near- or far-field [11]. Near-field sources apply EM induction or resonance methods for power transfer. For example, a sensor powered via near field communication (NFC) by a smart phone was presented in [12]. However, near-field harvesting might limit scaling for WSNs distributed over a wide area [11]. Far-field sources (range up to few kilometres) are for instance cellular base stations, TV stations or WiFi access points [1]. The available energy in the far field depends on the harvesting device's location and surroundings. Kinetic harvesters convert motions or vibrations into electrical energy via

electromagnetic [13–15], electrostatic [16–20] or piezoelectric [21–23] transduction methods [1]. Electromagnetic (EM) harvesters consist of magnets and coils. Based on Faraday's law, a varying magnetic flux induces an electric voltage across the coil [2]. The induced voltage depends on the number of the coil's turns as well as the size of coil and magnet. Thus, achieving small harvesters with a high power output is tough [19]. Applications with high amplitudes and low frequencies are suitable for EM harvester [24]. Piezoelectric harvesters utilise the piezoelectric effect to transduce mechanical into electrical energy when stress is applied on the geometry [2]. Electrostatic harvester exploit the ambient motion (for instance vibrations) to vary the distance of charged capacitor plates, resulting in a changing capacitance and thus energy transfer [2]. Ambient mechanical energy occurs in different forms such as rotation or vibration. Therefore, various harvester designs and techniques for these forms exist. Three-dimensional printed EM harvesters utilising rotation are presented in [25–30]. Three-dimensional printed EM vibration harvesters are reviewed in this paper. Furthermore, a recent review on various techniques for mechanical energy harvesting was provided in [31].

To achieve a higher energy output, different techniques or sources may be combined in hybrid harvesters [1]. Figure 1 shows the energy sources and their combinations. Combining multiple sources achieves multiple opportunities for energy harvesting (EH).

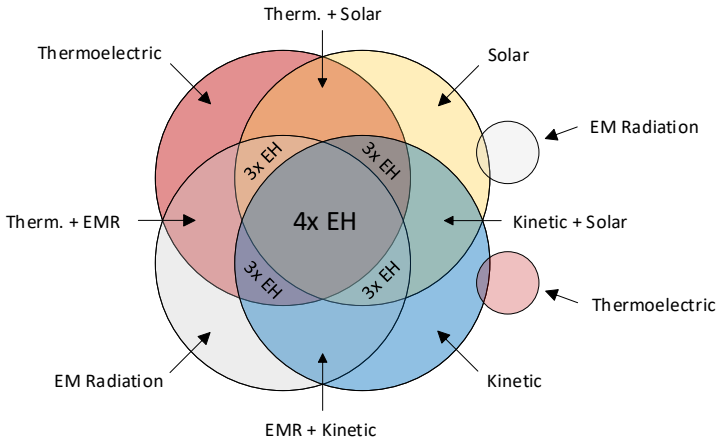

Figure 1. Energy sources and combinations.

2. 3D Printing

Additive manufacturing (AM) offers many benefits compared to traditional technologies such as moulding. The development is faster due to the seamless transfer from 3D Computer-Aided Design (CAD) to AM. No moulds are required, meaning different variants can be produced without additional costs and fabricating complex shapes requires no additional process steps [32]. Furthermore, AM has the potential of waste-, lead time- and cost-reduction. Assembled parts with relative motion can be printed together when utilising soluble support material and appropriate clearance between the parts [33]. Studies addressing the drawback of mass production capability along with opportunities such as mass customisation have been reported [34,35]. Printed harvesters either utilise the AM-process to print the housing of the harvester or to print functional parts such as springs or magnets of the device. Three-dimensional printing is also capable of printing multiple materials [36] at once as well as functional materials [37,38]. Three-dimensional printing or AM-processes apply the layer-by-layer-principle to create three-dimensional objects from 3D CAD-models [33]. There are seven AM-categories, each containing different technologies [32,33]. In this section, the most common printing techniques applied for energy harvesting devices are described: Binder jetting, fused filament fabrication and inkjet. Table 1 summarises the advantages and disadvantages of these three printing technologies.

2.1. Fused Filament Fabrication

Fused filament fabrication (FFF, also known as FDM) is categorised as material extrusion and utilises plastic filament which is melted in the hot end and then extruded through a nozzle onto the printing bed [33,37]. Figure 2a displays the process. As presented in the study common materials are PLA, ABS or PC but also advanced materials such as PVDF or PEEK. There is also the opportunity to utilise functional materials such as conductive filament to print electronic circuits [39].

Table 1. Advantages and disadvantages of Fused filament fabrication (FFF), Inkjet, Binder Jetting (BJT).

Technology	Advantages	Disadvantages
FFF	• Multi-material printing [33] • Functional materials available [39] • Printing assembled, movable parts (soluble support material) [33]	• Building speed [32] • Accuracy [32] • Surface roughness (depending on layer height) [33] • Material density [32]
Inkjet	• Multi-material-capabilities [33] • High layer-resolution (10–30 µm) [33] • High speed [32] • High scalability [32]	• High absorption of electromagnetic waves for photoactive compounds [33] • Limited choice of materials [32] • Lower accuracy for large parts [32]
BJT	• Large build volumes (up to 4 m in length) [32] • No support material required [32] • Combination of powder and binder-additives [32] • Fast printing process [32] • Various materials available (metal, polymer, ceramic, composite) [32] • Appropriate for low to medium batch production [32]	• Post processing required (infiltration) [32] • Lower accuracy than inkjet [32] • Poor surface finish [32]

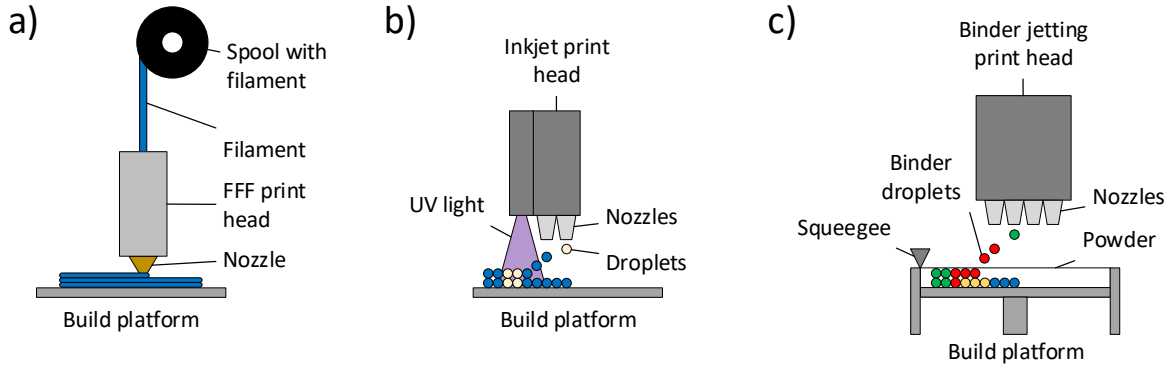

Figure 2. Schematic printing processes, (**a**) FFF with one extruder, (**b**) inkjet with photopolymers (blue = model material, beige = support material), (**c**) binder jetting with multiple colours.

2.2. Inkjet

Inkjet is a material jetting-process that utilises print heads with arrays of nozzles to eject material (for instance photopolymers, metals or ceramics) onto the print bed [32,33,37]. As showed in Figure 2b UV light is applied to cure the printed photopolymers and support-material. In addition, high layer-resolutions and multi-material-capabilities are mentioned for this process [33].

2.3. Binder Jetting

Binder Jetting (BJT), as described in [32], applies binder droplets to form the geometry for each powder-layer as well as to bond it to prior layers. Materials mentioned for BJT are,

for instance, plaster, metal or polymers. As stated in the monograph, the BJT print heads consist of multiple, parallel nozzles offering a fast and scalable process. Figure 2c displays the process. According to the authors, a post processing is necessary, which involves removing the part from the bed as well as remaining powder from the part. Infiltration or sintering may be used to improve the part's properties, depending on the material [32].

3. Review Methodology

3.1. Objective of the Review

The goal of this review is to provide a compact overview of the current printed vibration harvesting approaches, their principle of operation, the applied printing technique, the utilised materials, achieved power output, the degree of exploitation of 3D printing technology as well as open challenges. Details on the most common printing techniques were shortly explained in the previous section. A dedicated review on 3D printed vibration harvesters was provided in [41] in 2016. The contained harvesters were picked up in this review and extended with presented research from 2016 on.

3.2. Categories of Harvesters

The review is divided into non-hybrid and hybrid harvesters. Additionally, the harvesters are categorised based on their shape, resulting in tube-shaped, spherical, cantilevers, pendulum and others.

3.3. Formal Rules

As a blueprint for the review, [42] was applied. The search period was from 2016 to 2021. The latest search was carried out in September 2021. The reviewed literature was gathered via IEEE Xplore, SCOPUS and by checking the references of reviewed papers for relevant literature. The keywords applied were 3D printing, 3D printed, energy harvester, energy harvesting, electromagnetic, vibration.

3.4. Criteria for Exclusion

The EM harvester's central parts have to be 3D printed, except the coil and magnet. Meaning the printed parts should have an active function other than just offering a simple housing. For example, a harvester consisting of a printed spring with non printed coil and magnet is considered a "printed harvester" in this work. On the other hand, if the same harvester would utilise a non printed spring (e.g., wound steel wire) with just a printed housing, it is no longer considered a printed harvester. Printed parts offering a guiding-function as well as acting as housing (for instance a tube guiding a magnet ball) are considered active as well. However, few remarkable approaches found during the review process are presented in a dedicated section instead of being excluded. These papers might provide useful ideas or inspiration for new EM vibration harvesters.

4. 3D Printed Non-Hybrid Vibration Harvester

This section presents non-hybrid harvesters categorised by their shape.

4.1. Tube-Shaped

In [43], a vibration harvester with magnetic levitation was proposed. The device consisted of a cylindrical housing made of PLA, four magnets and a coil (1000 turns). Figure 3 shows the schematic and the printed harvester. Two magnets (NdFeB N35) were fixed the cylinders ends. The remaining two magnets (NdFeB N45) acted as inertial mass. They were glued together with a spacer between and faced each other with their north pole. The coil was wound around the cylinder. Under vibration, the inertial mass's movement induced a voltage in the coil. Guide rails inside the cylinder decreased the fraction between magnets and cylinder. The reported power output at resonance frequency of 10 Hz with 0.5 g was 1.4 mW with a 500 Ω load. A giant magnetoimpedance (GMI) accelerometer was

implemented with the harvester. In order to achieve a self-powered sensor, the authors aimed to expand the harvester's bandwidth for a better overall energy conversion.

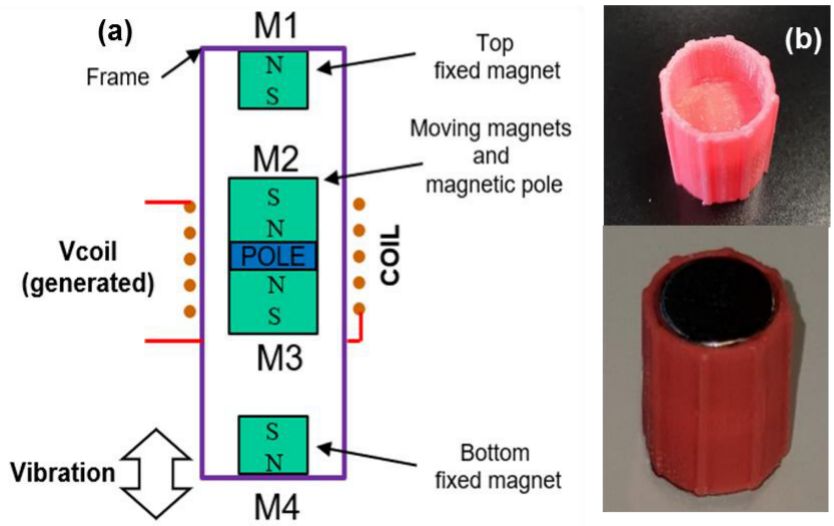

Figure 3. (**a**) Schematic of a straight tube harvester with magnetic springs [43], (**b**) printed harvester made of PLA with and without magnets [43].

In [44], a vibrational harvester was printed via inkjet (3D Systems ProJet 3510, materials: Visijet M3 Crystal and S300). The harvester was made of a printed body with a centred pad for a seismic mass. The pad was attached via springs printed in-plane. Multiple variants of spring geometries and thickness were tested. One or two magnets (1.5 mm diameter, 1 mm height) were placed on the central pad. A 7.36 mH SMD 812 coil was positioned 2 mm above the magnets as inductor. Figure 4 shows the harvester with one variant of the spring geometry as well as it's dimensions. The spring-geometry had a significant impact on the achievable voltage. 23.7 µW at a resonant frequency of 100 Hz were shown as the highest power output with a circular shaped spring. The harvester's reported total volume was less than 1 cm^3.

In [45], a linear tube-shaped, magnetic repulsion harvester was presented. Since the repulsive force between magnets is not linear such systems showed a non-linear frequency response. The authors exploited this to broaden the utilisable frequency range. The tube's inner surface showed the characteristic ridges from 3D printing. These increased the friction between tube and magnet-stack. In consequence, the authors turned the next prototype and did not print it. They also applied a ferrofluid to the magnet to reduce the friction. This improved the coupling between magnets and coils and thus increased the harvester's performance by 15%. Drilled magnets were applied as end caps to act as magnetic spring and improve the air flow affected by the ferrofluid. However, the authors pointed out that there were evaporation issues with the ferrofluid and that a sealed container might solve this. Five coils with 350 or 1400 turns in total were mounted on the tube. With a 75 Ω load, they calculated around 60 µW power output.

In [46], a 3D printed wrist-wearable harvester for human frequencies $\leq$5 Hz was reported. A hollow cycloid tube, printed with PLA, contained a 10 mm NdFeB N35 magnet ball. Two serially connected coils (600 turns each) were wrapped around the tube. A cycloid shape offered a shorter travel time of the ball from one end to the other, thus increasing the induced voltage into the coils. The authors also investigated straight and circular structures with the cycloid structure providing a 1.3 or 1.45 times higher open circuit voltage, respectively. The device was tested with a custom built swinging arm under 5 Hz excitation frequency and 2.5 g acceleration. The average power output was 8.8 mW with a 104.7 Ω load at 5 Hz. Vibrating hand motion of 5 s duration a wristwatch could be powered for 34 min.

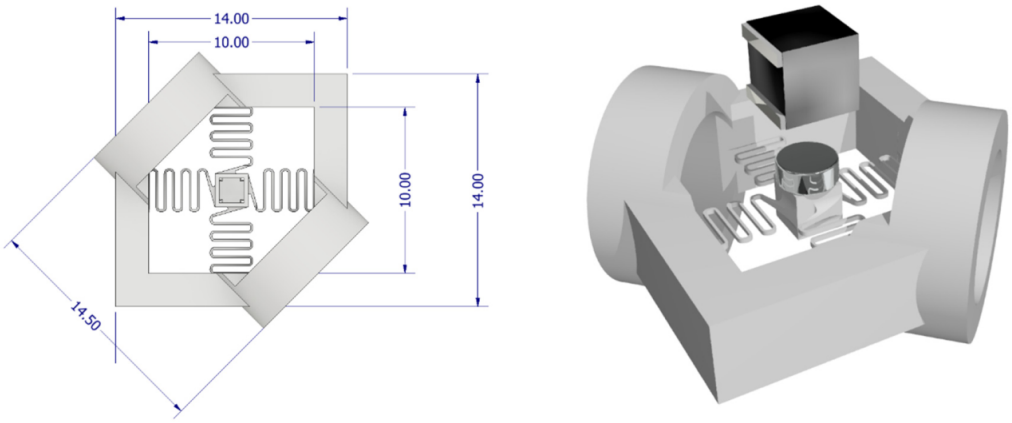

Figure 4. (**left**) Top view of inkjet printed harvester with dimensions in mm [44], (**right**) harvester with magnet and coil [44].

In [47], tube harvesters with 2 degrees of freedom (2-DOF) were investigated. The authors combined springs as linear and magnets as non-linear oscillators in four configurations to realise a 2-DOF harvester. The structure consisted of an outer tube containing an inner tube. The inner tube had a magnet (10 mm diameter and 10 mm thickness) inside. The magnet was either supported with springs or magnets. The inner tube itself was supported either with springs or magnets, resulting in four possible combinations. The tubes were printed via UV curable resin and had a coil (170 turns) wound around. All magnets were made of NdFeB. The authors pointed out that differences in their results between simulation and experiment might come due to intermittent sliding contact between magnet and tube because of the tube's deviation from vertical direction or from assembly. Configuration C with magnetic springs for the outer tube and linear springs for the magnet inside the inner tube was reported with a power output of 5.9 mW at 0.5 g. Configuration A with two linear springs showed 6.1 mW at 0.5 g.

In [48], a straight tube harvester was proposed. The authors applied a cylindrical N52 magnet and utilised the whole tube's surface for the coils. The harvester's dimensions were 14 mm in diameter and 50 mm in height (standard AA cell battery). An total of 6 mm in height was reserved for a future power management. The 0.5 mm thick tube was printed with resin and had 3 mm holes in the top and bottom for air flow. Different numbers of coils were investigated with four coils showing the best results. The average power output with four coils was 63.9 mW at 5 Hz hand shaking which equalled a power density of 9.42 mW/cm^3). A total of 4.2 mW was achieved when the harvester was worn at the ankle at 1 Hz walking. Connecting the coils in series or subtractive series decreased the power output.

In [49], a tube-like harvester with magnetic springs was proposed. Two NdFeB N35 magnets were attached to both ends of the printed hollow tube with a coil (480 turns) wrapped around the middle of tube. A stack consisting of two magnets was able to move inside the tube. The available length for the stack's movement as well as the stack's mass were adjustable and therefore allowed to tune the resonance frequency. For the stack, the magnets were orientated with opposite poles facing each other which was shown to provide a higher magnetic flux. The authors investigated combinations of lengths (140 mm or 200 mm) and magnet stacks consisting of either three or six magnets under different conditions. The harvester was attached to the leg of a participant either vertically or transversely while exposed to different walking speeds. The maximum power output of 10.66 mW was under running conditions with the combination of 200 mm length and a six magnets-stack. The authors mentioned the higher mass of the stack shifted the resonance frequency more towards the human motion frequency.

In [50], a magneto-mechanical device was reported. The harvester was based on a straight tube design, composed of a printed cylindrical housing with magnetic springs located at the top and bottom end and a coil wrapped around the centre. The end-magnets were mounted on bolts to adjust their distance. The moving NdFeB disc-magnet was fixed with four oblique springs (made of rubber) to the housing in order to vertically align it and prevent flipping. The oblique springs reduced the energy loss due to friction between magnet and walls as well as increased the non-linearity of the harvester. The housing had air vents for a better airflow and thus reduction in viscous damping. Three-dimensional printing material HIPS was applied via FFF. The maximum power was around 7 mW at 15 Hz with a 1.14 kΩ load and 0.75 g.

In [24], a vibration harvester was reported. It consisted of a group of magnets (adhesive force: 17 kg; weight: 18.8 g) on a bar, attached to a printed spring (diameter: 50 mm). These components were placed inside a cone-like structure with a coil (300 turns, 2.39 Ω) wrapped around its top. The spring caused the magnet to move up and down along the cone-structure's axis. The used material was ABS and the printer a X400 PRO 3D. Human motions with low frequency and high amplitude (8–16 Hz; 2.842–31.5827 m/s^2) were targeted—walking or running in particular. Therefore, the harvester was intended to be attached in the area under the knee. Different spirals were tested. Power outputs of 12–76 mW_{rms} at resonance with 8–15 Hz and a 2 Ω load were achieved. A decreasing output voltage during the 30 min test-cycle and a shift of the resonance frequency towards lower values were shown by the results. The geometry of the spring or the ABS's mechanical properties were pointed out as possible areas to be investigated in this regard.

4.2. Cantilever

In [51], a spiral micro array coil, a multipole magnet thin-plate and a 3D printed cantilever were utilised to create a micro-electromechanical system (MEMS) harvester. The magnet (8.9 mm × 8.9 mm, thickness 0.5 mm) had 16 poles with a chess pattern for an alternating magnetisation-direction. The coil array had 24 coils connected in series with a total resistance of 5.38 Ω and 144 turns. Both the multipole magnet and the coil array were fabricated by the authors. In one experiment, they 3D printed a 65 mm long cantilever made of PLA via FFF. The multipole magnet was attached to the cantilever while the coil remained fixed. An amount of 3.34 µW was reported as power output and 5.22 µW cm^{-3} as power density at 38 Hz and 11.6 g.

In [52], a coreless, non-linear, resonant vibration harvester was presented. The authors intended to improve the efficiency of coreless harvesters. They optimised the distribution of the coil's windings, resulting in fewer turns required and thus a higher power output. Figure 5 shows the harvester's magnets and coils. The two coils were racetrack-shaped with two times three magnets arranged between them. The magnets were split into four fixed (outer ones) and two movable ones (inner magnets). The latter were mounted on a cantilever, being deflected under vibrations and thus resulting in a varying magnetic flux. Due to optimisation, the coil's design had 746 turns (optimised) compared to 2000 turns (non optimised, uniformly distributed). An increase of 300% regarding the power output was achieved. The maximum power output was 6.46 mW at 35.5 Hz. A printing process or material were not mentioned. Based on the provided pictures, FFF was assumed as the process.

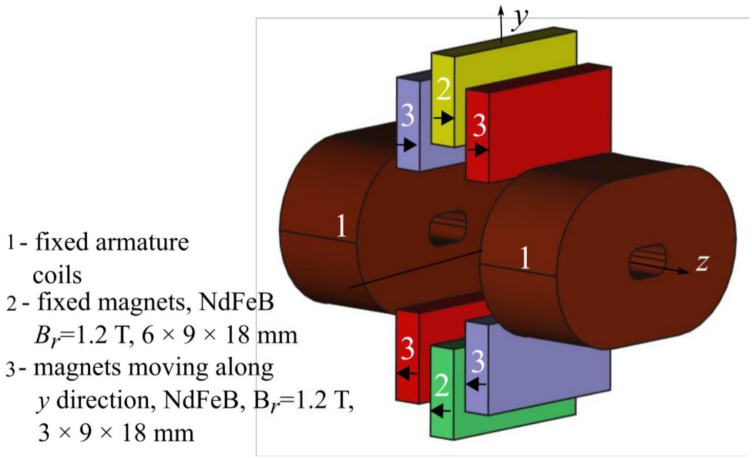

Figure 5. Magnets and coils from proposed harvester [52].

4.3. Pendulum

In [53], a non-linear pendulum-harvester was proposed. A cylindrical geometry with 12 symmetrically mounted coils (six on each side made of 28 AWG) and a pendulum with a permanent NdFeB N37 magnet in the middle was presented. Figure 6 shows the schematic of the pendulum. The authors connected the coils in series in order to achieve a high voltage-response of the harvester. Additional repulsive magnets were installed in some coils. Three-dimensional printing with ABS material was utilised to avoid magnetic coupling between the housing-geometries and magnets. As mentioned in the paper, a power output around 10 mW at 15 Hz was achieved. The authors pointed out that additional tests have to be carried out with higher values for the load resistor or excitation-frequency, but that was hindered by design constraints.

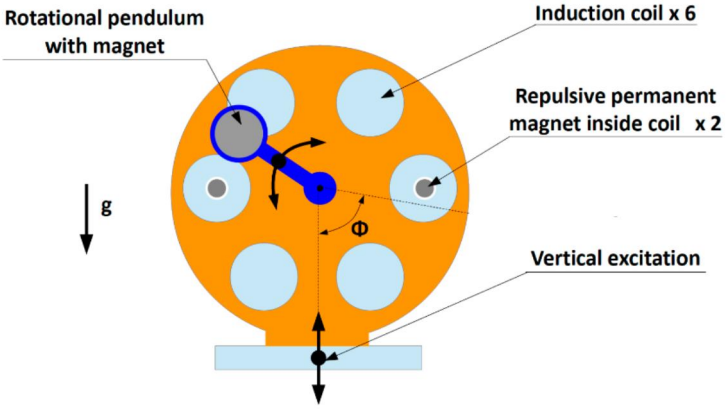

Figure 6. Pendulum-harvester schematic [53].

In [54], an inkjet printed pendulum-based harvester in a wrist watch housing was reported. The harvester was composed of the pendulum with eight integrated neodymium magnets, a disk with mounted SMD coils and a housing. The pendulum was attached to the disk and housing with a bearing. A Projet 3510 printer was utilised with Visijet M3 Crystal and S300 as model material and support material, respectively. The device provided a maximum peak-to-peak voltage of 1.8 V.

4.4. Others

In [55], a 3 degree of freedom (3-DOF) serial manipulator-type harvester was presented. The device was composed of a coil holder and three serially connected leaf hinge joints with a proof mass attached to the free end. The proof mass had three pairs of magnets

integrated and the coil holder contained a pair of concentric coils (1400 turns each). The harvester was printed with a Dimension SST1200ES 3D printer and ABSplus. In order to harvest multiple frequencies the device had three resonance frequencies at 23.4, 29.2, and 34.8 Hz. Based on the measured peak-to-peak voltages across the optimal load of 1.01 kΩ the peak powers were 1.28, 0.89 and 1.32 mW at an acceleration of 1.5 m/s^2. The normalized power density was reported as 2.85 kg s m^{-3}.

In [41], a non linear in-plane vibration harvester with a leaf isosceles trapezoidal flexural (LITF) pivot topology was presented. The out-of-plane motion was restricted by the LITF topology. FFF was applied to print the harvester's topology. The used printer was a Stratasys Mojo with ABS. NdFeB N35 magnets were glued to the movable tip and on the opposite of the frame. Between this arrangement, a coil (7060 turns, air core) was fixed to the stationary part. Mechanical energy was converted to the electrical domain once the structure was exposed to vibrations. Maximum power output was achieved at the resonance frequency. A power output of 2.9 mW (down sweep) was shown at 1 g. The authors emphasised the superiority of 3D printing for the monolithic fabrication of LITF pivot topologies. A review on 3D printed vibration harvesters as well as a review on (non 3D printed) in-plane harvesters were presented too.

In [56], the vibrations of a flying moth were harvested. The moth showed an available amplitude of 1 mm at 25 Hz measured on its back surface. A EM multi-phase AC generator was applied to harness the available energy. On the back of the moth, an FFF-printed ABS pedestal-structure was attached. Three NdFeB magnets (each 9.5 mm × 1.8 mm, 0.3 mm thick) and a core (0.2 mm thick) were held on the tip of the structure. Two magnet-core-assemblies faced each other with an air gap between. The PCB-windings utilised Kapton as substrate and were located in the air gap. Each of the three coils had two windings in a figure eight design on the double sided substrate. The generator had a total mass of 1.28 g. Tests were carried out with the generator attached on a shaker. A 1.7 mW power output into the load was reported with a shaker-amplitude of ±0.37 mm at 25.8 Hz and 0.9 mW with ±0.23 mm at 25.8 Hz.

In [57], a non-resonant vibration harvester was presented. It consisted of a printed housing with a spherical cavity containing a NdFeB magnet ball. The parameters (e.g., coil turns, cavity diameter) were varied for testing. Depending on the variant one or two copper coils were wound around the device. The goal was to harness human motion in different conditions (walking/running). The housing was printed via binder jetting with powder/resin on a Spectrum Z510 3D printer. A better power output was shown with two coils placed with an offset to the cavity's equator. A power output of 1.44 mW was achieved by a variant placed in the pocket (offset wound coil with 500 turns). The highest shown power density was 0.5 mW/cm^3.

In [58], a resonance-based vibration harvester was printed via FFF and ABS material. The first generator was based on assembled aluminium parts fixed with screws. Screws were not suitable in a vibrating environment the authors pointed out. Therefore, FFF (Dimension BST) was utilised to print ABS-parts for the generator. Epoxy glue was applied to connect the printed parts. A lever with a magnetic circuit at its tip induced a voltage in a fixed coil due to Faraday's law. The lever's stiffness was tuned via permanent magnets repelling a magnet on the lever. Printing offers parts with low weight and durability according to the authors. The generator operated at 17 Hz with an amplitude of 0.1–1 g. The maximum power output was 26 mW with 9 V (DC). The harvester's size was 80 × 60 × 60 mm^3. It is not clear if the lever was printed or made of non-printed material. The latter would meet the criteria for exclusion of this paper.

Table 2 summarises the non-hybrid harvesters for later discussion.

Table 2. 3D printed electromagnetic non-hybrid vibration harvesters in the literature.

Ref.	Year	Structure	Power in mW	Energy Source	Special Feature
[51]	2021	Cantilever	3.34×10^{-3}	Low frequency vibrations	MEMS harvester
[43]	2020	Straight tube	1.4	Low frequency vibrations	Self-powered accelerometer
[53]	2020	Pendulum	10	Mechanical vibrations (shaker)	Oscillations and rotations possible
[44]	2020	Cubic tube	2.37×10^{-2}	Mechanical vibrations	Total volume less than 1 cm^3
[52]	2020	Cantilever	6.46	Shaker	Optimised coil windings
[45]	2019	Straight tube (1)	6×10^{-2}	Environment with low frequency + high amplitude	Ferrofluid as lubricant
[46]	2019	Cycloid tube	8.8	Human motion wrist or foot	Optimised shape of harvester
[47]	2019	Straight tube	6.1	Shaker	2-DOF harvester
[55]	2019	Manipulator type	$1.28_{(23.4\ Hz)}$ (p) $0.89_{(29.2\ Hz)}$ (p) $1.32_{(34.8\ Hz)}$ (p)	Shaker	3-DOF harvester with leaf hinge joints
[54]	2019	Pendulum	-	Wrist movement	Inkjet printed harvester
[48]	2018	Straight tube	63.9	Human hand shaking	Coils all over surface
[49]	2017	Straight tube	10.66	Human leg motion	Magnetic spring
[50]	2017	Straight tube	7 (p)	Shaker	Oblique springs for alignment
[41]	2016	LITF pivot	2.9 (ds)(p)	Mechanical vibrations	Topology restricts out of plane movement
[24]	2016	Straight tube	76	Human motion (walking)	Printed spring
[56]	2009	3D spring	1.7	Vibrations from flying moth	Harvesting energy from moth
[57]	2008	Spherical	1.44	Random human motion	Multi-direction harvesting
[58]	2008	Moving arm	26	Ambient mechanical vibration	Repelling magnets as oscillator

(1) final prototype not 3D printed (ds) down sweeps values (p) peak power.

5. 3D Printed Hybrid Vibration Harvester

Hybrid harvester combine multiple energy sources and/or harvesting principles, for instance solar and kinetic sources or piezo and electromagnetic transducers. Figure 1 shows possible combinations of energy sources.

5.1. Tube-Shaped

In [59], a 3D printed tube contained a magnet attached to a spring, an electromagnetic generator (EMG), a contact separation mode triboelectric nanogenerator (CTENG) and a sliding mode triboelectric nanogenerator (STENG). An aluminium (Al) strip was wrapped around the magnet for the STENG. Two coils were mounted around and the STENG's electrodes inside the tube. The CTENG was located in the bottom. As explained by the authors, once the magnet started oscillating a voltage was induced in the coil by Faraday's law, a triboelectric charge transfer was induced in the STENG and the CTENG was compressed in the magnets lowest position. The maximum peak power outputs were 717 mW at 600 Ω for the EMG, 18.9 mW at 2 MΩ for the CTENG and 1.7 mW at 6 MΩ for the STENG. The device's regulated DC power output was 34.11 mW.

In [60], a non resonant impact based harvester with a similar structure as in [59] was presented. A magnet with two springs on its top and bottom was inside a printed rectangular tube with a coil mounted in the centre as EMG. Two CTENGs were integrated with their positive and negative triboelectric material on the open ends of the springs as well as the tube's bottom and ceiling, respectively. The magnet started oscillating once the device was under excitation. According to the paper a soft magnetic film was utilised as flux-concentrator for the EMG on the coil's outside. This increased the induced voltage in the coil by 1.39 times. Furthermore a dry lubricant was applied to the coils frame for easier

magnet-movement. The harvester's power output was 144.1 mW with a load of 1.5 kΩ at 6 Hz and 1 g.

In [61], a springless hybrid, non resonant harvester was proposed. An EMG and four triboelectric nanogenerators (TENG) (two contact mode and two sliding mode) were combined. The EMG utilised a dual-Halbach array (NdFeB N52) for an increased magnetic flux density and a coil (460 turns). The TENG-materials were PTFE and Al. The harvester's structure was a bobbin with the coil inside a hollow, 3D printed frame for the Halbach-arrays with a distance of 1.2 mm between coil and magnets. On the outside of the Halbach-frame Al-electrodes were mounted. Around the bobbin and Halbach-frame another frame was located with PTFE-film and cooper electrode attached. Bobbin and outer frame were attached, the Halbach-frame could freely slide inside. Excitation of the device caused the Halbach-frame to slide back and forth along the axis. Thus, electromagnetic induction in the coil as well as electrostatic induction in the sliding mode TENG occurred. The contact mode TENGs were active when the Halbach-frame slid back after touching the ends of the outer frame. The transformer was attached to the TENGs and a multiplier circuit to the EMG in order to achieve a combined, regulated output for the device. Since no spring was applied in the harvester, it showed different power outputs when applied horizontally or vertically due to gravity. The horizontal power output on a Shaker at 6 Hz and 1 g was 5.41 mW with a 1.1 KΩ load. Vertically, 3.28 mW was achieved. The device was also tested under human motions such as handshaking, walking or slow running and delivered up to 2.9 mW. The authors mentioned wearable and portable devices as applications for the harvester.

In [62], a 3D printed wrist-wearable hybrid harvester for human frequencies $\leq$5 Hz was reported. A hollow curved tube, printed with ABS contained an EMG and TENG. The former consisted of a 10 mm NdFeB N52 magnet ball and two serially connected coils wrapped around the tube. The latter utilised the ABS-tube and the ball as triboelectric material with a PTFE-film between, inside the tube. Al-electrodes were wrapped outside around the tube. The PTFE-ABS composite was applied because the voltage generated just with ABS was not high enough and more suitable materials such as PTFE were not available for 3D printing. Only ABS resulted in a peak-to-peak voltage around 7.5 V. Applying a nano-structured PTFE-film achieved around 20 V. The power density was reported with 5.14 mW cm^{-3} with 49.2 Ω load for the EMG and 0.22 µW cm^{-3} with 13.9 MΩ for the TENG between 3 and 4 Hz. The harvested energy from 5 s running was enough to power an electric wrist watch for 410 s.

In [63], an improved version of [62] was reported. A broader range of human motion patterns could be exploited to harvest energy. The hybrid device combined electromagnetic and triboelectric generators to harvest human wrist motion such as shaking, twisting or waving with $\leq$5 Hz. The harvester's structure was a 3D printed circular hollow tube made of PLA. The EMG composed of four serially connected coils (300 turns each) evenly distributed and wound around the tube as well as a 10 mm magnet ball inside. A FeSiCr/PDMS-film was wrapped around the coils as flux concentrator to enhance the EMG. Simulations showed that the concentrator increased the flux density from 0.577 T to 1.168 T. The TENG composed of a PTFE-film inside the PLA-tube, four Al-electrodes wrapped around the tube and the magnet ball. The TENG's capabilities were also enhanced; for example, the ball was treated with grit abrasive paper to achieve a micro-structured surface. At 4–5 Hz excitation frequency and a 100 Ω load the EMG had an average power output of 3.46 mW without and 4.98 mW with the flux concentrator. The TENG achieved 0.0058 µW at 12 MΩ on average without and 93 nW with the PTFE-film.

5.2. Spherical

In [64], a multi-direction, low-frequency hybrid device to harvest the motion of waves was presented. The showed harvester with a cylindrical shape was on based on an EMG and a TENG. Four S-shaped TENGs in the bottom supported a printed curved surface above. A magnetic ball was enclosed inside the housing while being able to freely move

around on the curved surface. Above the ball's area a coil (1500 turns) was located. Inside the curved surface a free-standing mode TENG was embedded which utilised the ball as positive tribolayer. The authors exploited this to measure the direction and amplitude based on the balls movement. Furthermore, the moving ball caused deformation of the supporting S-shaped contact-separation TENGs (CTENG) as well as a varying magnetic flux through the coil. The maximum power output at 1 Hz were 3.65 mW for the S-shaped TENGs and 22.4 mW for the EMG. The authors also demonstrated a self-powered seawater splitting system and a self-powered electrochemical cathodic protection system with the harvester.

In [65], a spherical hybrid harvester was presented as self-powered six axis inertial sensor for hand motion recognition as well as monitoring human activity. The authors combined electromagnetic, piezoelectric and triboelectric transducers in the device along with multiple magnetic balls inside the hollow 3D printed sphere. All generators were implemented in the shell of the sphere with wound wire or films. The device was characterised by vibrating it periodically along its x-axis with an amplitude of 26 cm. The EMG's two coils with 91 buckyballs had a power output of 13.8 nW and 22.4 nW with loads of 25 Ω and 20 Ω at a frequency around 2.5 Hz. The two piezoelectric films had a power output of 0.12 µW and 0.19 µW with loads of 10 MΩ at circa 2.5 Hz. The triboelectric generator's films showed 0.22 µW and 0.72 µW at 12 MΩ and 15 MΩ at approximately 3 Hz. The overall power output was not mentioned and is, therefore, not shown in Table 3.

5.3. Pendulum

In [66], a non-resonant hybrid EMG-TENG harvester for ultralow frequencies was proposed. The harvester had a printed cylindrical shell (white resin) with a vertical pendulum inside. The pendulum was similar to a metronome but flexible into all directions. The pendulum's shaft consisted of a spring with a printed, hollow rod around to increase its stiffness. The shaft was fixed to the shell at the bottom and on the top end a magnet (Ø 22 mm × 20 mm) was attached. Above the magnet a coil was attached onto the shell's ceiling and four TENGs were attached to the inner walls of the cylindrical shell. The TENGs were designed with a double helix structure made of copper-foil and FEP-film. When exposed to external excitation the pendulum with the magnet started swinging around, inducing a voltage into the coil due to Faraday's law of induction. When the magnet collided with the TENG's the layers were pressed together, achieving temporary contact, thus resulting in triboelectrification. At 2.2 Hz, the peak power output for the EMG was 523 mw at 280 Ω and for the TENG 470 µW at 0.5 MΩ. A wireless temperature sensor was driven by the harvester and a LTC3106 as power management.

In [67], a piezo-electromagnetic hybrid-harvester with frequency up-conversion was reported. Figure 7 (left) illustrates the harvester's structure. A rotating mass block with integrated magnets was attached via a bearing to a shaft with four cantilevers. Piezo-elements were glued on the cantilevers surface. On the cantilevers' free end, NdFeB magnets were mounted, facing coils (200 turns each) attached to the fixed base. The mass block and the base were 3D printed with PLA. Under excitation the mass block started swinging. When a magnet on a cantilever's free end was passed by a magnet in the mass block, the cantilever was excited in its natural frequency of 42 Hz. Due to this structure frequency up-conversion was provided. The magnets mounted on the cantilevers caused a varying magnetic flux through the coils, resulting in an induced voltage due to Faraday's law. The reported peak power outputs were 1.28 mW for the piezo, 30 µW for the EMG and 1.31 mW when both were coupled. Figure 7 right shows the experimental setup with the printed harvester attached to a shaker.

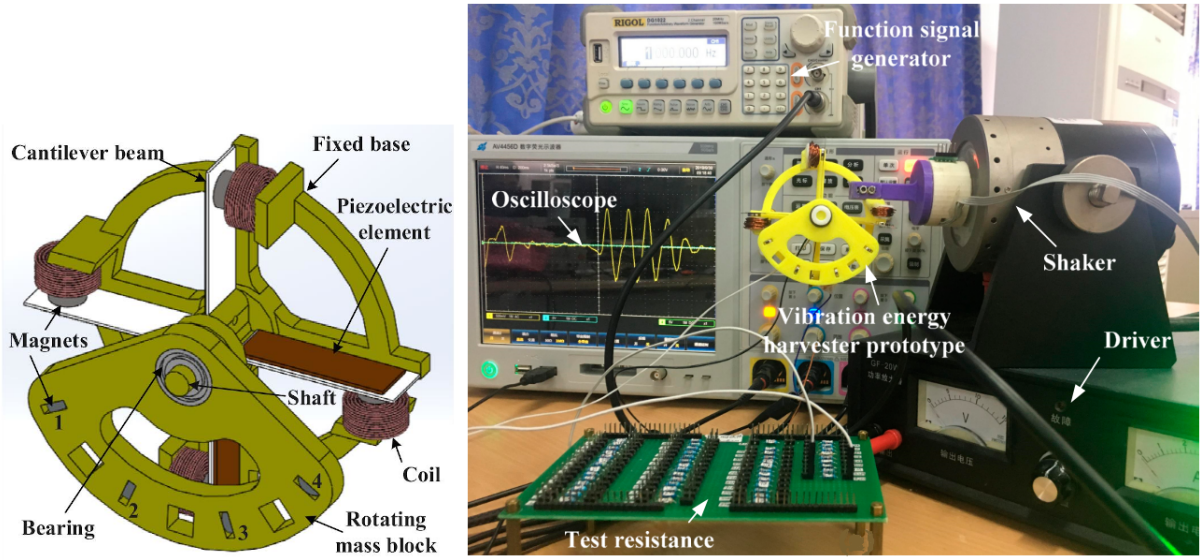

Figure 7. (**left**) Structure of the hybrid piezo-electromagnetic multi-directionalharvester [67], (**right**) experimental setup with printed harvester [67].

5.4. Others

In [68], a hybrid electromagnetic (EMG) and triboelectric nanogenerator (TENG) with three axis motion sensing capabilities was proposed. The vibration harvester's geometry consisted of a central cylinder with four arms symmetrically distributed around made of printed PLA. Inside the centre and each arm, slidable magnets were integrated. At the outer end of the arms, fixed magnets were attached. Coils were located on the top and bottom (1200 turns each) of the centre as well as wound around each arm (500 turns each). Due to repulsion from the centre-magnet the movable magnets were pushed towards the outer end. The TENG, made of micro-structured PTFE film, Al film and copper electrodes, was implemented in the centre's bottom. Due to the moving magnets, a voltage was induced in the coils (EMG) and a charge transfer occurred due to the sliding frictional effect (TENG). The peak power output were 18 mW with 193 Ω for the EMG and 3.25 µW with 10.5 MΩ load for the TENG. The reported resonance-frequency was 7 Hz. The Combination of EMG and TENG increased the voltage of a charged capacitor by around 50% compared to the EMG alone. A version printed with PLA with a higher power output (27 mW EMG and 56 µW TENG) was shown by the same authors in [69].

Table 3. 3D printed electromagnetic hybrid vibration harvesters in the literature.

Ref.	Year	Structure	Combination	Power in mW	Energy Source	Special Feature
[66]	2021	Pendulum	EMG	523 (p)	Blue energy	Multi-direction pendulum
			TENG	0.47 (p)		
[69]	2020	Cross shape	EMG	27 (p)	In-plane motions and vibrations	Linear/rotational motion sensor
			TENG	5.6×10^{-2} (p)		
[64]	2020	Cylinder/	EMG	22.4 (p)	Random low frequency	Vibration amplitude sensor
		spherical	TENG	3.65 (p)	vibrations	
[59]	2020	Straight tube	EMG, TENG	34.11	Human motion, ocean waves, automotive vibration	Universal self-chargeable power module

Table 3. *Cont.*

Ref.	Year	Structure	Combination	Power in mW	Energy Source	Special Feature
[60]	2020	Straight tube	EMG, TENG	144.1	Human motion	Universal power source
[67]	2020	Pendulum	Piezo	1.28 $^{(p)}$	Human motion,	Frequency up-conversion
			EMG	3×10^{-2} $^{(p)}$	low frequency vibrations	
[68]	2019	Cross shape	EMG	18 $^{(p)}$	In-plane motions and vibrations	Linear/rotational motion sensor
			TENG	3×10^{-3} $^{(p)}$		
[65]	2019	Spherical	EMG, Piezo, TENG	-	Human motion	Six axis inertial sensor
[61]	2018	Straight tube	EMG, TENG	5.41	Human induced vibration	Springless harvester
[62]	2018	Curved tube	EMG, TENG	-	Human motion	Wrist wearable harvester
[63]	2018	Circular tube	EMG	4.98	Human wrist motion	Flux concentrator
			TENG	9.3×10^{-5}		

Note: If a dedicated power output was given for EMG, TENG or piezo they were separated by a line break. $^{(p)}$ peak power.

6. Considerable Fields of Investigation for Future Vibration Harvesters

In this section, a few compression harvesters as well as some other interesting approaches are listed. For instance, multi-direction-harvesting, functional materials or microorganism-harvesting. These might provide inspiration and impulses to adapt functionalities in order to create new approaches or improvements for vibration harvesting.

6.1. Compression

In [70], a spherical multi-direction harvester with a moulded silicone-shell was presented. The devices core was printed with PLA with guiding tubes for two integrated magnet balls. Coils were mounted around the tubes. Figure 8 shows the harvester's internal structure. The authors applied a compressible silicone-shell. Under compression, the shell actuated olive oil, which then forced the magnet balls to move, thus passing a coil and inducing a voltage. Once the deformation of the shell was gone, the fluid flowed back into its original location and pushed the balls into the opposite direction through the coil. This combination of shell and fluid allowed the multi-directional actuation. Olive oil was applied due to its high viscosity to move the balls. A less viscous fluid such as water would flow around the balls without moving them. The harvester was tested under frequencies of 4–15 Hz and achieved between 17 and 44 mV.

In [71], a harvester was presented, which translated compression from human walking (linear movement) into a rotary motion. Once compressed, the harvester kept rotating inertially. The housing of the device was 3D printed. The device applied a twisted steel rod. Due to compression, the rod actuated a ratchet-pawl-combination and the rotor started spinning. A spring pulled the rotor back up to the starting position. While rotating the eight NdFeB N52-magnets on the rotor and four fixed coils (400 turns each) converted mechanical energy to the electrical domain according to Faraday's law. A power output of 11 mW at 0.84 Hz and 85 Ω load was achieved. The harvester was also integrated into a shoe to harvest human motion. Under running conditions (9 km/h), a power output of 85 mW was observed.

In [72], a rectangular piece of magnetostrictive material (2826 MB) was embedded inside an FFF printed bone, made of PLA. Around the bone a collector coil (4000 turns, 0.385 mm wire diameter) was attached along with a bias NdFeB magnet ($150 \times 20 \times 10$ mm^3). The external magnet was necessary to provide a working magnetic field. Applied axial stress applied to the bone caused a compression of the magnetostrictive material and therefore a change of its permeability due to the Villari effect. Thus, the magnetic flux

density changed and induced a voltage in the coil according to Faraday's law. Various human walking-conditions were simulated for testing. The maximum harvested power was 0.1 mW during simulated quick running.

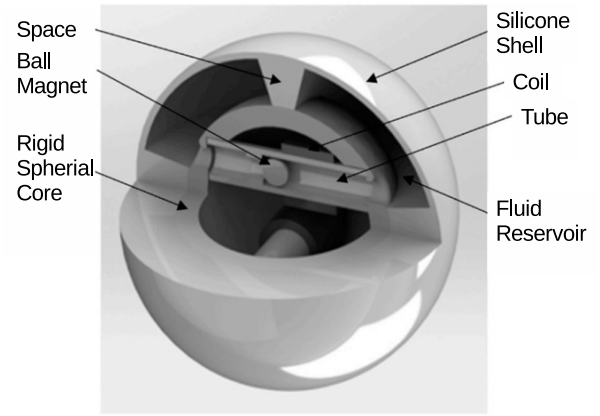

Figure 8. Image showing the harvester's internal structure [70].

6.2. Others

In [73], a rotational harvester with a 3D printed magnet was proposed for energy harvesting from power transmission lines. The NdFeB-magnet was made of compound material Neofer 25/60p. It was printed via FFF on a low-cost 3D printer. The magnet was mounted on a shaft with two bearings, which were fixed in a frame. A coil (750 turns) was wound around the frame. Two devices were built and tested in a two axis Helmholtz coil platform. A DC bias magnetic field was required for centring the magnet in its equilibrium position. An AC magnetic field then induced a rotary movement of the magnet. One device's magnet has been topologically optimised in order to achieve a more homogeneous radial magnetic field. The optimised magnet was recessed on two sides of its cylindrical shape. As a consequence, the distortion power factor of the optimised harvester increased by 55%. However, the power output decreased by 25% due to the lower magnet volume. At resonance, a power output of 93 mW with a 10 Ω load was achieved. The applied DC magnetic field had an impact on the device's resonance frequency. Applications mentioned were wireless sensor networks and IoT.

An interesting approach was presented in [74], where micro-organisms (phytoplankton and zooplankton) were utilised to power 3D printed actuation mechanisms. The movement of the micro-organisms was controlled by geometric forms as well as external stimuli. Phototaxis as one kind of stimulus caused micro-organisms to move towards (positive) or away from (negative) a light source. A linear movement was been achieved with a printed float with a fin beneath and matured Artemia sallina. The fin separated a channel with blue LEDs on both ends. If the LED was turned on, the negative phototaxis organisms escaped from it. They collided with the fin and pushed it to the opposite direction. With 50 Artemia, an average speed of 0.21 mm/s and a driving force of 0.537 mN were observed. This equalled 0.11 mW per organism. For practical application, a higher number of Artemia would be necessary. A rotary movement of 0.4 rpm was achieved with a printed ratchet and 300 Artemia in their larva-stage (positive phototaxis). The ratchet was printed on KEYENCE AGILISTA-3100 (inkjet) and AR-M2 (UV cureable resin) as material. A mask was applied to cause positive phototaxis movement around the ratchet. A ratchet made by photolithography was also tested with another organism (Volvox). Two ratchet-designs were tested and obtained—0.86 rpm and 2.01 rpm. A conversion from the kinetic into the electric domain has not been implemented.

7. Discussion

Table 2 summarises the reviewed non-hybrid harvesters. The first printed vibration harvesters (based on the criteria of this review) were presented in 2008. Figure 9 shows the distribution regarding the shape. Tube-like harvesters (straight or circular) are the biggest category while other categories are rather evenly distributed. The power outputs of the harvesters vary from 3 µW to 76 mW. The power density would provide a good comparison, taking the size into account. However, the harvester's dimensions were not provided in most papers. Therefore, size or power density could not be investigated properly and were not listed in the tables. Figure 10 shows the output power grouped into <1 mW, from 1–10 mW and >10 mW with average and peak power separated. It can be seen that the majority of the non-hybrid harvesters fall into the range of 1–10 mW. The harvested energy sources are mostly human motions or mechanical vibrations. Regarding the special feature-column, there are various interesting topics, from miniaturisation to coil optimisation or expanding the harvester's degree of freedoms.

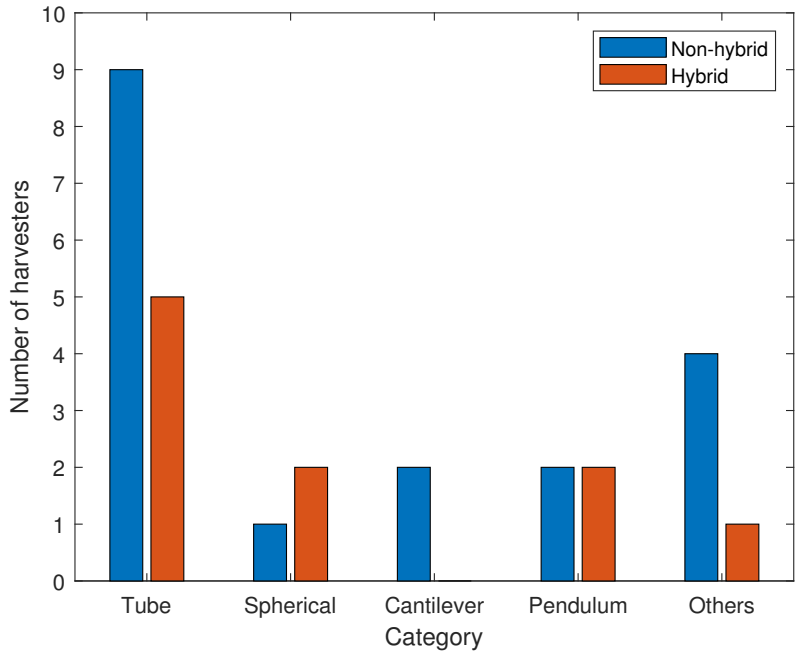

Figure 9. Bar graph with 3D printed EM hybrid and non-hybrid vibration harvesters grouped into categories.

Hybrid harvesters are presented in Table 3. A frequently applied shape is tube-like, as shown in Figure 9. EMG were mostly combined with TENG. Piezo-transducer were only utilised two times. Regarding the average power output, which was not given in some papers, 5 mW to 144 mW were found. The peak power outputs vary from around 1.3 mW to over 520 mW. The common targeted energy sources are human motions as well as low frequency vibrations such as blue energy. The special features are the exploitation of the harvester as sensor, utilisation of flux concentrators or multi-direction-harvesting.

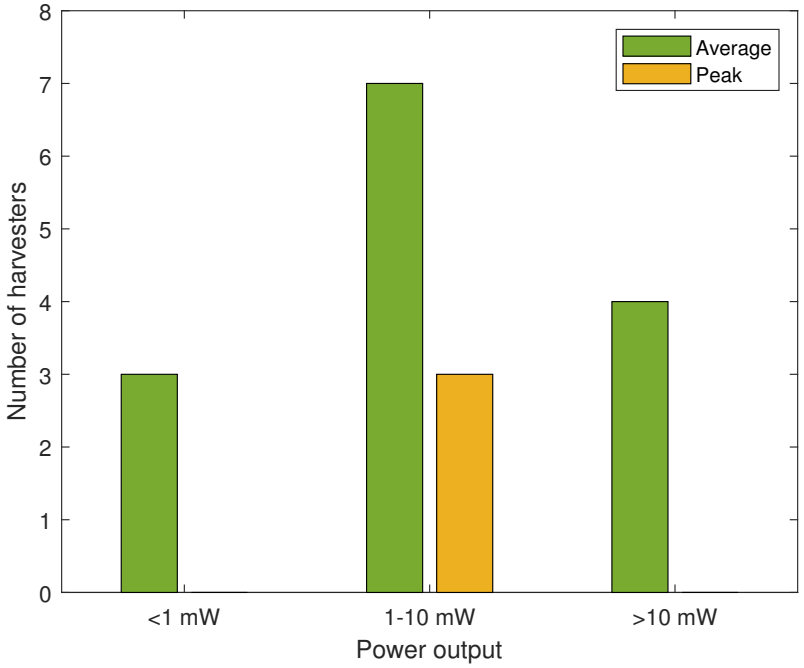

Figure 10. Bar graph with power outputs of 3D printed EM non-hybrid vibration harvesters grouped into three power classes.

7.1. Utilisation of 3D Printing

Tables 4 and 5 show the reviewed harvesters, the applied printing technology, the utilised material, the printed parts as well as the utilisation of 3D printing categorised by [41]. Binder jetting and FFF were applied first in 2008, while FFF was the most common process in the following years. Harvesters printed via inkjet came up quite recently. Inkjet offers better printing resolutions than FFF and therefore potential for miniaturised harvesters as seen in [44]. In some cases, the technology was not mentioned, but for ABS/PLA, it was most likely that FFF was utilised. As for materials ABS and PLA, these were printed most commonly for hybrid and non-hybrid, followed by resin-materials. It can be seen that none of the harvesters utilised functional materials, indicating a field worth investigating. Based on [41] utilising 3D printing for vibration harvesters can be categorised into fabricating support structures or suspension mechanisms. In [73], (rotational harvester) magnetic material was 3D printed for an optimised magnet topology in order to achieve a more homogeneous radial magnetic field. Other functional materials such as carbon fibre filaments or conductive materials could also offer benefits for vibration harvesters, their longevity or transducer mechanisms.

Table 4. Comparison of applied 3D printing techniques for electromagnetic vibration harvesters.

Ref.	Year	Structure	Process	Material	Printed Parts	Utilisation 3D Printing
[51]	2021	Cantilever	FFF	PLA	Cantilever	Suspension
[43]	2020	Straight tube	FFF	PLA	Tube	Support
[53]	2020	Pendulum	FFF (assumed)	ABS	Housing, pendulum	Support
[44]	2020	Cubic tube	Inkjet	Visijet M3 Crystal, S300	Spring, frame	Suspension
[52]	2020	Cantilever	FFF (assumed)	-	Cantilever, coil holder	Suspension
[45]	2019	Straight tube [(1)]	-	-	Tube	Support
[46]	2019	Cycloid tube	-	PLA	Tube	Support
[47]	2019	Straight tube	-	UV curable resin	Tube	Support
[55]	2019	Manipulator type	FFF	ABSplus	Main body, proof masses	Suspension
[54]	2019	Pendulum	Inkjet	Visijet M3 Crystal, S300	Housing, pendulum	Support
[48]	2018	Straight tube	-	Resin	Tube	Support
[49]	2017	Straight tube	-	-	Tube	Support
[50]	2017	Straight tube	FFF	HIPS	Housing	Support
[41]	2016	LITF pivot	FFF	ABS	Main body	Suspension
[24]	2016	Straight tube	FFF	ABS	Spiral/spring, housing	Suspension
[56]	2009	3D spring	FFF	ABS	3D spring	Suspension
[57]	2008	Spherical	Binder jet	Powder/resin	Housing	Support
[58]	2008	Moving arm	FFF	ABS	Immovable parts	Support

[(1)] final prototype not 3D printed.

Table 5. Comparison of applied 3D printing techniques for hybrid electromagnetic vibration harvesters.

Ref.	Year	Structure	Process	Material	Printed Parts	Utilisation 3D Printing
[66]	2021	Pendulum	-	Resin	Shell, magnet support, adjusting stud, rod	Support
[69]	2020	Cross shape	-	PLA	Body, covers	Support
[64]	2020	Cylinder	-	-	Disc, circular surface	Support
[59]	2020	Tube	-	PLA	Main hollow body	Support
[60]	2020	Tube	FFF (assumed)	ABS	Frame/Tube	Support
[67]	2020	Pendulum	-	PLA	Mass block, base	Support
[68]	2019	Cross shape	-	PLA	Body	Support
[65]	2019	Spherical	-	-	Shell	Support
[61]	2018	Tube	-	-	Housing	Support
[62]	2018	Curved tube	-	ABS	Tube	Support
[63]	2018	Circular tube	-	PLA	Tube	Support

7.2. Advantages of 3D Printing

Three-dimensional printing offers many advantages such as a faster, easier and cheaper process compared to traditional fabrication [46,54,62]. It is possible to create monolithically fabricated 3D structures in a single process [41] and, in general, complex structures are more feasible and cheaper to fabricate [62]. Furthermore, unintentional

electromagnetic coupling can be avoided with 3D printing materials [53]. Miniaturisation-opportunities have been shown for inkjet [44]. Taking a look outside the box, in [75] a triboelectric generator was realised with polyamide and the rubber-like material TangoBlack. Based on the work covered in this paper, the utilisation of multi-material-printing with such materials or others has not been found. Therefore, multi-material-printing might be a field worth investigating for novel vibration generator designs.

7.3. Disadvantages of 3D Printing

In [45], small ridges from printing resulted in an increase in the friction coefficient. Based on the printing technique, material, layer resolution, orientation in the build camber as well as the printed geometry itself, the characteristic transitions from layer to layer could be an issue. Possible solutions are presented in the following section. Regarding hybrid harvesters/TENGs, certain materials (such as PTFE) offering better performance are not available yet [62]. In [24], a performance-decrease in the harvester's printed spring during testing was observed. Therefore, the long-term behaviour of printed materials in regard to their application should be considered. Simulations regarding stress and fatigue for 3D printed harvester parts should be investigated as well. Regarding inkjet, the high absorption of electromagnetic waves for photoactive compounds mentioned in [33] should be examined.

7.4. Enhancing Performance

In order to increase the harvester's power output in [63] a FeSiCr/PDMS-film was wrapped around the coils as flux concentrator. Simulations showed that the concentrator increased the flux density from 0.577 T to 1.168 T. In [45], ridges caused by the layer-stacking when printing were a drawback of 3D printing. In [47], intermittent sliding contact might have caused differences between experiment and simulation. Three-dimensional printing was not mentioned as reason, but reducing the surface's friction might improve the harvesters performance. In [60], a dry lubricant was applied to counter this issue. In [49], graphite powder was used as lubricant to reduce the friction and in [43] guide rails were utilised. In [50], a reduction in viscous damping was achieved with holes in the housing to improve the airflow. Furthermore, oblique springs were applied to align the magnet [50].

7.5. Applications

There are various applications mentioned; specific applications as well as potential fields of application. The most common fields are WSNs [44,52,58,66] as well as wearables/portable devices [24,46,54,62,63]. Health/fitness monitoring [62,63] are a subcategory of wearables. For WSNs, animal monitoring [54], forest monitoring [54] or environmental monitoring [64] are named. Specific applications in the field of portable devices are a self-chargeable power module [59] and a universal power source [60]. Furthermore, a self-powered seawater splitting system [64] and a self-powered electrochemical cathodic protection system [64] are mentioned. A very promising development is the exploitation of the harvester directly as sensor [64,65,68,69].

8. Conclusions

This review summarised the 3D printed EM vibration harvesters over the past 13 years. An introduction with the different energy harvesting categories and their combination was presented. The applied methodology for the review was explained. A total of 18 different 3D printed non-hybrid and 11 different hybrid harvesters were reviewed, compared and discussed. Maximum average power outputs of 76 mW (non-hybrid) and 144 mW (hybrid) were found. The tube-shape was the most applied geometry. A dedicated analysis on the utilisation of 3D printing for vibration harvesters was conducted. It has been shown that 3D printing is suitable to manufacture vibration harvesters. FFF was the most applied printing technology for non-hybrid and hybrid vibration harvesters. Research gaps were

derived with multi-material-printing, functional materials or multi-directional harvesting as well as movement–conversion approaches. Furthermore, micro-organism-harvesting could be a future field of research. Applications for printed harvesters were gathered and listed. Finally, the remaining challenges and opportunities are summarised; challenges are the following:

- Finding miniaturisation strategies for harvesters utilising FFF.
- Identifying more strategies for FFF to overcome the drawback of the characteristic surface-ridges.
- Investigating the long-term behaviour of 3D printed suspensions and potential differences between the printing techniques in this regard.
- Examining the effect of photoactive compounds on electromagnetic waves for inkjet.

Arising opportunities are the following:

- The monolithic printing of harvesters.
- No dependency on additional tools or moulds, thus quick realisation of variants.
- Fabricating complex and filigree structures.
- Faster and easier production than with traditional techniques and, therefore, mass customisation capabilities. This allows for tailoring the harvester specifically towards the application's surrounding conditions.
- Printing multiple materials in one process as well as the availability of functional materials and materials without electromagnetic coupling.
- Miniaturisation with inkjet (volumes less than 1 cm^3).

Author Contributions: P.G. is the lead author of this review. He conceptualised, investigated and wrote the original version of this paper. T.M.W., L.S., N.H. and U.B.H. contributed by reviewing the paper and T.M.W. by project administration. All authors have read and agreed to the published version of the manuscript.

Funding: The article processing charge was funded by the Baden-Württemberg Ministry of Science, Research and Culture and the Offenburg University of Applied Sciences in the funding programme Open Access Publishing.

Institutional Review Board Statement: Not applicable.

Informed Consent Statement: Not applicable.

Data Availability Statement: The raw data of graphs presented in this review are available on request from the corresponding author.

Conflicts of Interest: The authors declare no conflict of interest.

Abbreviations

The following abbreviations are used in this manuscript:

ABS	Acrylonitrile Butadiene Styrene
AM	Additive Manufacturing
AWG	American Wire Gauge
BJT	Binder Jetting
CAD	Computer-Aided Design
CTENG	Contact-separation Mode Triboelectric Nanogenerator
DC	Direct Current
DOF	Degree Of Freedom
EH	Energy Harvesting
EM	Electromagnetic
EMG	Electromagnetic Generator
FDM	Fused Deposition Modeling
FEP	Fluorinated Ethylene Propylene

FFF	Fused Filament Fabrication
HIPS	High Impact Polystyrene
LITF	Leaf Isosceles Trapezoidal Flexural
MEMS	Microelectromechanical System
NFC	Near Field Communication
PDMS	Polydimethylsiloxane
PLA	Polylactic Acid
PTFE	Polytetrafluoroethylene
RF	Radio Frequency
STENG	Sliding Mode Triboelectric Nanogenerator
TEG	Thermoelectric Generator
TENG	Triboelectric Nanogenerator
WSN	Wireless Sensor Node

References

1. Ku, M.L.; Li, W.; Chen, Y.; Ray Liu, K.J. Advances in Energy Harvesting Communications: Past, Present, and Future Challenges. *IEEE Commun. Surv. Tutor.* **2016**, *18*, 1384–1412. [CrossRef]
2. Elvin, N.; Erturk, A. *Advances in Energy Harvesting Methods*; Springer: New York, NY, USA, 2013. [CrossRef]
3. Tang, L.; Yang, Y.; Soh, C.K. Toward Broadband Vibration-based Energy Harvesting. *J. Intell. Mater. Syst. Struct.* **2010**, *21*, 1867–1897. [CrossRef]
4. Chien, L.J.; Drieberg, M.; Sebastian, P.; Hiung, L.H. A simple solar energy harvester for wireless sensor networks. In Proceedings of the 2016 6th International Conference on Intelligent and Advanced Systems (ICIAS), Kuala Lumpur, Malaysia, 15–17 August 2016; pp. 1–6. [CrossRef]
5. Senivasan, S.; Drieberg, M.; Singh, B.S.M.; Sebastian, P.; Hiung, L.H. An MPPT micro solar energy harvester for wireless sensor networks. In Proceedings of the 2017 IEEE 13th International Colloquium on Signal Processing Its Applications (CSPA), Penang, Malaysia, 10–12 March 2017. [CrossRef]
6. Kokert, J.; Beckedahl, T.; Reindl, L.M. Medlay: A Reconfigurable Micro-Power Management to Investigate Self-Powered Systems. *Sensors* **2018**, *18*, 259. [CrossRef] [PubMed]
7. Pubill, D.; Serra, J.; Verikoukis, C. Harvesting artificial light indoors to power perpetually a Wireless Sensor Network node. In Proceedings of the 2018 IEEE 23rd International Workshop on Computer Aided Modeling and Design of Communication Links and Networks (CAMAD), Barcelona, Spain, 17–19 September 2018; pp. 1–6.
8. Ma, X.; Bader, S.; Oelmann, B. Characterization of Indoor Light Conditions by Light Source Classification. *IEEE Sens. J.* **2017**, *17*, 3884–3891. [CrossRef]
9. Verma, G.; Sharma, V. A Novel Thermoelectric energy harvester for Wireless Sensor Network Application. *IEEE Trans. Ind. Electron.* **2019**, *66*, 3530–3538. [CrossRef]
10. Moser, A.; Erd, M.; Kostic, M.; Cobry, K.; Kroener, M.; Woias, P. Thermoelectric Energy Harvesting from Transient Ambient Temperature Gradients. *J. Electron. Mater.* **2012**, *41*, 1653–1661. [CrossRef]
11. Yedavalli, P.S.; Riihonen, T.; Wang, X.; Rabaey, J.M. Far-Field RF Wireless Power Transfer with Blind Adaptive Beamforming for Internet of Things Devices. *IEEE Access* **2017**, *5*, 1743–1752. [CrossRef]
12. Boada, M.; Lazaro, A.; Villarino, R.; Gil, E.; Girbau, D. Near-Field Soil Moisture Sensor with Energy Harvesting Capability. In Proceedings of the 2018 48th European Microwave Conference (EuMC), Madrid, Spain, 23–27 September 2018; pp. 235–238. [CrossRef]
13. Liu, H.; Hou, C.; Lin, J.; Li, Y.; Shi, Q.; Chen, T.; Sun, L.; Lee, C. A non-resonant rotational electromagnetic energy harvester for low-frequency and irregular human motion. *Appl. Phys. Lett.* **2018**, *113*, 203901. [CrossRef]
14. Tan, Y.; Dong, Y.; Wang, X. Review of MEMS Electromagnetic Vibration Energy Harvester. *J. Microelectromechanical Syst.* **2017**, *26*, 1–16. [CrossRef]
15. Wang, L.; Todaria, P.; Pandey, A.; O'Connor, J.; Chernow, B.; Zuo, L. An Electromagnetic Speed Bump Energy Harvester and Its Interactions With Vehicles. *IEEE/ASME Trans. Mechatronics* **2016**, *21*, 1985–1994. [CrossRef]
16. Pourshaban, E.; Karkhanis, M.U.; Deshpande, A.; Banerjee, A.; Ghosh, C.; Kim, H.; Mastrangelo, C.H. Flexible Electrostatic Energy Harvester Driven by Cyclic Eye Tear Wetting and Dewetting. In Proceedings of the 2021 IEEE International Conference on Flexible and Printable Sensors and Systems (FLEPS), virtually, 20–23 June 2021; pp. 1–4. [CrossRef]
17. Qian, Y.; Yu, J.; Zhang, F.; Kang, Y.; Su, C.; Pang, H. Facile synthesis of sub-10 nm ZnS/ZnO nanoflakes for high-performance flexible triboelectric nanogenerators. *Nano Energy* **2021**, *88*, 106256. [CrossRef]
18. Qian, Y.; Lyu, Z.; Kim, D.H.; Kang, D.J. Enhancing the output power density of polydimethylsiloxane-based flexible triboelectric nanogenerators with ultrathin nickel telluride nanobelts as a co-triboelectric layer. *Nano Energy* **2021**, *90*, 106536. [CrossRef]
19. Zhang, Y.; Wang, T.; Luo, A.; Hu, Y.; Li, X.; Wang, F. Micro electrostatic energy harvester with both broad bandwidth and high normalized power density. *Appl. Energy* **2018**, *212*, 362–371. [CrossRef]
20. Aljadiri, R.T.; Taha, L.Y.; Ivey, P. Electrostatic Energy Harvesting Systems: A Better Understanding of Their Sustainability. *J. Clean Energy Technol.* **2017**, *5*, 409–416. [CrossRef]

21. Yuan, X.; Gao, X.; Yang, J.; Shen, X.; Li, Z.; You, S.; Wang, Z.; Dong, S. The large piezoelectricity and high power density of a 3D-printed multilayer copolymer in a rugby ball-structured mechanical energy harvester. *Energy Environ. Sci.* **2020**, *13*, 152–161. [CrossRef]
22. Thakare, N.S.; Thakare, S.S.; Shahakar, R.S. Recent Advancement and Comparative Performance Analysis of Energy Harvesting Technique. In Proceedings of the 2018 Second International Conference on Intelligent Computing and Control Systems (ICICCS), Madurai, India, 14–15 June 2018; pp. 1631–1634. [CrossRef]
23. Zhao, J.; You, Z. A shoe-embedded piezoelectric energy harvester for wearable sensors. *Sensors* **2014**, *14*, 12497–12510. [CrossRef] [PubMed]
24. Garcia-Moreno, P.; Perez, M.E.; Estevez, F.J.; Gloesekoetter, P. Study of Wearable and 3D-Printable Vibration-Based Energy Harvesters. In Proceedings of the 2016 15th International Conference on Ubiquitous Computing and Communications and 2016 International Symposium on Cyberspace and Security (IUCC-CSS), Granada, Spain, 14–16 December 2016; pp. 101–108. [CrossRef]
25. Herawan, S.G.; Syahputra, S.A.; Tokit, E.M.; Sa'at, F.A.Z.M.; Rosli, M.A.M. Effect of number of permanent magnetic poles on 3D printed coreless generator rotor. *IOP Conf. Ser. Mater. Sci. Eng.* **2021**, *1082*, 012009. [CrossRef]
26. Herawan, S.G.; Syahputra, S.A.; Tokit, E.M.; Sa'at, F.A.Z.M.; Rosli, M.A.M. Energy harvesting applications using 3D-printed coreless generator. *IOP Conf. Ser. Mater. Sci. Eng.* **2021**, *1082*, 012004. [CrossRef]
27. Soemphol, C.; Angkawisittpan, N. 3D-printed materials based low-speed permanent magnet generator for energy harvesting applications. *Mater. Today Proc.* **2020**, *22*, 180–184. [CrossRef]
28. Adamski, K.T.; Adamski, J.W.; Urbaniak, L.; Dziuban, J.A.; Walczak, R.D. 3D Printed Miniature Water Turbine with Integrated Discrete Electronic Elements for Energy Harvesting and Water Flow Measurement. *J. Phys. Conf. Ser.* **2018**, *1052*, 012086. [CrossRef]
29. Lee, J.; Jeon, G.; Kim, S. Magnetically axial-coupled propeller-based portable electromangetic energy-harvesting device using air and water stream. In Proceedings of the 2018 IEEE International Magnetics Conference (INTERMAG), Singapore, 23–27 April 2018; p. 1. [CrossRef]
30. Han, N.; Zhao, D.; Schluter, J.U.; Goh, E.S.; Zhao, H.; Jin, X. Performance evaluation of 3D printed miniature electromagnetic energy harvesters driven by air flow. *Appl. Energy* **2016**, *178*, 672–680. [CrossRef]
31. Maamer, B.; Boughamoura, A.; Fath El-Bab, A.M.; Francis, L.A.; Tounsi, F. A review on design improvements and techniques for mechanical energy harvesting using piezoelectric and electromagnetic schemes. *Energy Convers. Manag.* **2019**, *199*, 111973. [CrossRef]
32. Gibson, I.; Rosen, D.; Stucker, B.; Khorasani, M. *Additive Manufacturing Technologies*, 3rd ed.; Springer: Cham, Swizterland, 2021. [CrossRef]
33. Calignano, F.; Manfredi, D.; Ambrosio, E.P.; Biamino, S.; Lombardi, M.; Atzeni, E.; Salmi, A.; Minetola, P.; Iuliano, L.; Fino, P. Overview on Additive Manufacturing Technologies. *Proc. IEEE* **2017**, *105*, 593–612. [CrossRef]
34. Chen, T.C.T.; Lin, Y.C. A three-dimensional-printing-based agile and ubiquitous additive manufacturing system. *Robot. Comput.-Integr. Manuf.* **2019**, *55*, 88–95. [CrossRef]
35. Darwish, L.R.; El-Wakad, M.T.; Farag, M.M. Towards sustainable industry 4.0: A green real-time IIoT multitask scheduling architecture for distributed 3D printing services. *J. Manuf. Syst.* **2021**, *61*, 196–209. [CrossRef]
36. Junk, S.; Gawron, P.; Schröder, W. Development of an Additively Manufactured Adaptive Wing Using Digital Materials. In *Sustainable Design and Manufacturing*; Ball, P., Huaccho Huatuco, L., Howlett, R.J., Setchi, R., Eds.; Springer: Singapore, 2019; pp. 49–59.
37. Wendt, T.; Hangst, N.; Gawron, P.; Junk, S. 3D-Druck von leitfähigen Materialien bei gedruckter Sensorik in intelligenten und multifunktional aufgebauten Mensch-Roboter-Kollaborations-Greifsystemen: 3D-Printing of Conductive Materials by Printed Sensors in Intelligent and Multifunctional Human-Robot-Collaboration-Grippers. In *Sensors and Measuring Systems*; VDE: Frankfurt am Main, 2018; pp. 135–138.
38. Wendt, T.; Gawron, P.; Hangst, N. Conductive materials and 3D printing—An overview. In *LOPEC Conference Proceedings 2019*; Messe München GmbH: München, 2019.
39. Flowers, P.F.; Reyes, C.; Ye, S.; Kim, M.J.; Wiley, B.J. 3D printing electronic components and circuits with conductive thermoplastic filament. *Addit. Manuf.* **2017**, *18*, 156–163. [CrossRef]
41. Constantinou, P.; Roy, S. A 3D printed electromagnetic nonlinear vibration energy harvester. *Smart Mater. Struct.* **2016**, *25*, 095053, doi:10.1088/0964-1726/25/9/095053.
41. Constantinou, P.; Roy, S. A 3D printed electromagnetic nonlinear vibration energy harvester. *Smart Mater. Struct.* **2016**, *25*, 095053. [CrossRef]
42. Pautasso, M. Ten simple rules for writing a literature review. *PLoS Comput. Biol.* **2013**, *9*. [CrossRef]
43. Beato-López, J.J.; Royo-Silvestre, I.; Algueta-Miguel, J.M.; Gómez-Polo, C. A Combination of a Vibrational Electromagnetic Energy Harvester and a Giant Magnetoimpedance (GMI) Sensor. *Sensors* **2020**, *20*, 1873. [CrossRef] [PubMed]
44. Kawa, B.; Śliwa, K.; Lee, V.C.; Shi, Q.; Walczak, R. Inkjet 3D Printed MEMS Vibrational Electromagnetic Energy Harvester. *Energies* **2020**, *13*, 2800. [CrossRef]
45. POROBIC, I.; GONTEAN, A. Electromagnetic energy harvester. In Proceedings of the 2019 IEEE 25th International Symposium for Design and Technology in Electronic Packaging (SIITME), Cluj-Napoca, Romania, 23–26 October 2019; pp. 151–154. [CrossRef]

46. Maharjan, P.; Bhatta, T.; Salauddin Rasel, M.; Salauddin, M.; Toyabur Rahman, M.; Park, J.Y. High-performance cycloid inspired wearable electromagnetic energy harvester for scavenging human motion energy. *Appl. Energy* **2019**, *256*, 113987. [CrossRef]
47. Fan, K.; Liang, G.; Zhang, Y.; Tan, Q. Hybridizing linear and nonlinear couplings for constructing two–degree–of–freedom electromagnetic energy harvesters. *Int. J. Energy Res.* **2019**, *5*, 041306. [CrossRef]
48. Zhao, X.; Cai, J.; Guo, Y.; Li, C.; Wang, J.; Zheng, H. Modeling and experimental investigation of an AA-sized electromagnetic generator for harvesting energy from human motion: ACCEPTED MANUSCRIPT. *Smart Mater. Struct.* **2018**, *27*, 085008. [CrossRef]
49. Wang, W.; Cao, J.; Zhang, N.; Lin, J.; Liao, W.H. Magnetic-spring based energy harvesting from human motions: Design, modeling and experiments. *Energy Convers. Manag.* **2017**, *132*, 189–197. [CrossRef]
50. Nammari, A.; Caskey, L.; Negrete, J.; Bardaweel, H. Design and investigation of an enhanced magneto-mechanical nonlinear energy harvester. In *Active and Passive Smart Structures and Integrated Systems 2017*; Park, G., Ed.; SPIE: Bellingham, WA, USA, 2017; p. 101642K. [CrossRef]
51. Han, D.; Shinshi, T.; Kine, M. Energy Scavenging From Low Frequency Vibrations Through a Multi-Pole Thin Magnet and a High-Aspect-Ratio Array Coil. *Int. J. Precis. Eng. Manuf.-Green Technol.* **2021**, *8*, 139–150. [CrossRef]
52. Kulik, M.; Jagieła, M.; Łukaniszyn, M. Surrogacy-Based Maximization of Output Power of a Low-Voltage Vibration Energy Harvesting Device. *Appl. Sci.* **2020**, *10*, 2484. [CrossRef]
53. Ambrożkiewicz, B.; Litak, G.; Wolszczak, P. Modelling of Electromagnetic Energy Harvester with Rotational Pendulum Using Mechanical Vibrations to Scavenge Electrical Energy. *Appl. Sci.* **2020**, *10*, 671. [CrossRef]
54. Adamski, K.; Walczak, R. Pendulum base 3D printed electromagnetic energy harvester. *J. Phys. Conf. Ser.* **2019**, *1407*, 012114. [CrossRef]
55. Kim, H.S.; Ryu, W.; Park, S.b.; Choi, Y.J. 3-Degree-of-freedom electromagnetic vibration energy harvester with serially connected leaf hinge joints. *J. Intell. Mater. Syst. Struct.* **2019**, *30*, 308–322. [CrossRef]
56. Chan, S.C.; Yaul, F.M.; Dominguez-Garcia, A.; O'Sullivan, F.; Otten, D.M.; Lang, J.H. Harvesting energy from moth vibrations during flight. In Proceedings of the PowerMEMS 2009, Washington, DC, USA, 1–4 December 2009; pp. 57–60.
57. Bowers, B.J.; Arnold, D. Spherical Magnetic Generators for Bio-Motional Energy Harvesting. In Proceedings of the PowerMEMS 2008, Sendai, Japan, 9–12 November 2008; pp. 281–284.
58. Hadas, Z.; Zouhar, J.; Singule, V.; Ondrusek, C. Design of Energy Harvesting Generator Base on Rapid Prototyping Parts. In Proceedings of the 2008 13th International Power Electronics and Motion Control Conference, Poznań, Poland, 1–3 September 2008; pp. 1665–1669.
59. Maharjan, P.; Bhatta, T.; Cho, H.; Hui, X.; Park, C.; Yoon, S.; Salauddin, M.; Rahman, M.T.; Rana, S.S.; Park, J.Y. A Fully Functional Universal Self–Chargeable Power Module for Portable/Wearable Electronics and Self–Powered IoT Applications. *Adv. Energy Mater.* **2020**, *10*, 2002782. [CrossRef]
60. Rahman, M.T.; Rana, S.S.; Salauddin, M.; Maharjan, P.; Bhatta, T.; Park, J.Y. Biomechanical Energy–Driven Hybridized Generator as a Universal Portable Power Source for Smart/Wearable Electronics. *Adv. Energy Mater.* **2020**, *10*, 1903663. [CrossRef]
61. Salauddin, M.; Toyabur, R.M.; Maharjan, P.; Rasel, M.S.; Kim, J.W.; Cho, H.; Park, J.Y. Miniaturized springless hybrid nanogenerator for powering portable and wearable electronic devices from human-body-induced vibration. *Nano Energy* **2018**, *51*, 61–72. [CrossRef]
62. Maharjan, P.; Cho, H.; Rasel, M.S.; Salauddin, M.; Park, J.Y. A fully enclosed, 3D printed, hybridized nanogenerator with flexible flux concentrator for harvesting diverse human biomechanical energy. *Nano Energy* **2018**, *53*, 213–224. [CrossRef]
63. Maharjan, P.; Toyabur, R.M.; Park, J.Y. A human locomotion inspired hybrid nanogenerator for wrist-wearable electronic device and sensor applications. *Nano Energy* **2018**, *46*, 383–395. [CrossRef]
64. Yang, H.; Deng, M.; Zeng, Q.; Zhang, X.; Hu, J.; Tang, Q.; Yang, H.; Hu, C.; Xi, Y.; Wang, Z.L. Polydirectional Microvibration Energy Collection for Self-Powered Multifunctional Systems Based on Hybridized Nanogenerators. *ACS Nano* **2020**, *14*, 3328–3336. [CrossRef]
65. Koh, K.H.; Shi, Q.; Cao, S.; Ma, D.; Tan, H.Y.; Guo, Z.; Lee, C. A self-powered 3D activity inertial sensor using hybrid sensing mechanisms. *Nano Energy* **2019**, *56*, 651–661. [CrossRef]
66. Xie, W.; Gao, L.; Wu, L.; Chen, X.; Wang, F.; Tong, D.; Zhang, J.; Lan, J.; He, X.; Mu, X.; et al. A Nonresonant Hybridized Electromagnetic-Triboelectric Nanogenerator for Irregular and Ultralow Frequency Blue Energy Harvesting. *Research* **2021**, *2021*, 5963293. [CrossRef] [PubMed]
67. Shi, G.; Chen, J.; Peng, Y.; Shi, M.; Xia, H.; Wang, X.; Ye, Y.; Xia, Y. A Piezo-Electromagnetic Coupling Multi-Directional Vibration Energy Harvester Based on Frequency Up-Conversion Technique. *Micromachines* **2020**, *11*, 80. [CrossRef] [PubMed]
68. Bhatta, T.; Maharjan, P.; Park, J.Y. All-Direction In-Plane Magnetic Repulsion-Based Self-Powered Arbitrary Motion Sensor and Hybrid Nanogenerator. In Proceedings of the 2019 19th International Conference on Micro and Nanotechnology for Power Generation and Energy Conversion Applications (PowerMEMS), Kraków, Poland, 2–6 December 2019; pp. 1–4. [CrossRef]
69. Bhatta, T.; Maharjan, P.; Salauddin, M.; Rahman, M.T.; Rana, S.S.; Park, J.Y. A Battery-Less Arbitrary Motion Sensing System Using Magnetic Repulsion–Based Self–Powered Motion Sensors and Hybrid Nanogenerator. *Adv. Funct. Mater.* **2020**, *30*, 2003276. [CrossRef]
70. Hall, R.G.; Rashidi, R. Multi-Directional Universal Energy Harvesting Ball. *Micromachines* **2021**, *12*, 457. [CrossRef] [PubMed]

71. Luo, A.; Zhang, Y.; Xu, W.; Lu, Y.; Wang, F. Electromagnetic Energy Harvester with Inertial Rotary Structure for Human Motion Application at Ultra-Low Frequency. In Proceedings of the 2020 IEEE 33rd International Conference on Micro Electro Mechanical Systems (MEMS), Vancouver, BC, Canada, 18–22 January 2020; pp. 536–539. [CrossRef]
72. Tan, Y.; Zhang, Y.; Ren, L. Energy Harvesting From an Artificial Bone. *IEEE Access* **2019**, *7*, 120065–120075. [CrossRef]
73. Wang, Z.; Huber, C.; Hu, J.; He, J.; Suess, D.; Wang, S.X. An electrodynamic energy harvester with a 3D printed magnet and optimized topology. *Appl. Phys. Lett.* **2019**, *114*, 013902. [CrossRef]
74. Hatsuzawa, T.; Yanagida, Y.; Nisisako, T. Microorganisms driven micro actuation mechanisms for the kinetic energy harvesting. In Proceedings of the 2017 19th International Conference on Solid-State Sensors, Actuators and Microsystems (TRANSDUCERS), Kaohsiung, Taiwan, 18–22 June 2017; pp. 2067–2070. [CrossRef]
75. Haque, R.I.; Farine, P.A.; Briand, D. 3D Printed Materials Based Triboelectric Device for Energy Harvesting and Sensing. *Proceedings* **2017**, *1*, 580. [CrossRef]